

RESEARCH

Open Access



# Radiomics analysis in predicting vascular invasion in gastric cancer based on enhanced CT: a preliminary study

Zhicheng Chen<sup>1,3†</sup>, Guangfeng Zhang<sup>2,3†</sup>, Yi Liu<sup>4\*</sup> and Kexin Zhu<sup>3\*</sup>

## Abstract

**Background** Vascular invasion (VI) is closely related to the metastasis, recurrence, prognosis, and treatment of gastric cancer. Currently, predicting VI preoperatively using traditional clinical examinations alone remains challenging. This study aims to explore the value of radiomics analysis based on preoperative enhanced CT images in predicting VI in gastric cancer.

**Methods** We retrospectively analyzed 194 patients with gastric adenocarcinoma who underwent enhanced CT examination. Based on pathology analysis, patients were divided into the VI group ( $n = 43$ ) and the non-VI group ( $n = 151$ ). Radiomics features were extracted from arterial phase (AP) and portal venous phase (PP) CT images. The radiomics score (Rad-score) was then calculated. Prediction models based on image features, clinical factors, and a combination of both were constructed. The diagnostic efficiency and clinical usefulness of the models were evaluated using receiver operating characteristic (ROC) curves and decision curve analysis (DCA).

**Results** The combined prediction model included the Rad-score of AP, the Rad-score of PP, Ki-67, and Lauren classification. In the training group, the area under the curve (AUC) of the combined prediction model was 0.83 (95% CI 0.76–0.89), with a sensitivity of 64.52% and a specificity of 92.45%. In the validation group, the AUC was 0.80 (95% CI 0.67–0.89), with a sensitivity of 66.67% and a specificity of 88.89%. DCA indicated that the combined prediction model might have a greater net clinical benefit than the clinical model alone.

**Conclusion** The integrated models, incorporating enhanced CT radiomics features, Ki-67, and clinical factors, demonstrate significant predictive capability for VI. Moreover, the radiomics model has the potential to optimize personalized clinical treatment selection and patient prognosis assessment.

**Keywords** Gastric cancer, Multidetector computed tomography, Ki-67, Vascular invasion, Radiomics

<sup>†</sup>Zhicheng Chen and Guangfeng Zhang contributed equally to this work and share first authorship.

\*Correspondence:

Yi Liu

liuyicmu@sina.cn

Kexin Zhu

springzhuwork@163.com

<sup>1</sup>Department of Radiology, Shengjing Hospital of China Medical University, No.36 Sanhao Street, Heping District, Shenyang 100004, China

<sup>2</sup>Department of Radiology, Children's Hospital Affiliated to Shandong University, 23976 Jingshi road, Huaiyin District, Jinan 250000, China

<sup>3</sup>Department of Radiology, The First Hospital of China Medical University, 155 North Nanjing Street, Heping District, Shenyang 110001, China

<sup>4</sup>Department of Medical Imaging, Cancer Hospital of China Medical University, Liaoning Cancer Hospital & Institute, No.44 Xiaoheyuan Road, Dadong District, Shenyang 110042, China



## Background

Gastric cancer is one of the most common malignant tumors globally, ranking among the top five in incidence and mortality rates [1]. In particular, China accounts for 50% of the worldwide incidence and mortality of gastric cancer [2]. For resectable gastric cancer, surgery is considered the optimal treatment modality [3]. However, gastric cancer is characterized by a high rate of recurrence after surgery, which remains the primary cause of elevated postoperative mortality in these patients [4, 5]. It is essential to identify gastric cancer patients at high risk of recurrence early and to develop individualized treatment plans.

Vascular invasion (VI) is defined as the invasion of blood vessels by malignant tumor cells within the primary tumor and surrounding tissues [6]. VI is closely related to the metastasis, recurrence, prognosis, and treatment of gastric cancer [7]. Therefore, accurately assessing preoperative VI status is crucial for optimal clinical decision-making and personalized treatment [8]. Currently, predicting VI preoperatively using traditional clinical examinations alone remains challenging. Enhanced CT, a non-invasive diagnostic technique, enables visualization of tumor angiogenesis and is routinely performed as a preoperative examination [9]. With advancements in computer technology, radiomics based on enhanced CT has been widely used for differential diagnosis [10], staging [11, 12], preoperative evaluation [13, 14], and prognosis of gastric cancer [15, 16]. However, few radiomics studies focus on VI in gastric cancer [17]. Ki-67 is a nuclear non-histone protein expressed in all stages of cell proliferation except the G0 phase and can be used as a predictor of cell proliferation to predict the recurrence of gastric cancer [18]. Therefore, Ki-67 may be associated with the presence of VI in gastric cancer patients. In China, endoscopic biopsy before gastrectomy is a common clinical procedure, providing important information about the local part of the gastric tumor, such as Ki-67 and Lauren classification [19]. However, endoscopic biopsy has limitations as it cannot accurately reflect the biological behavior of the entire tumor.

This study aims to establish a radiomics prediction model based on preoperative enhanced CT combined with Ki-67 to explore its value in predicting VI in gastric cancer. This model aims to provide a new tool for evaluating prognosis and optimizing individualized treatment for gastric cancer patients.

## Patients and methods

### Participants

The retrospective study was approved by our institutional review board, and the requirement for informed consent was waived. Data were collected retrospectively for 503 gastric cancer patients admitted between January 2017

and May 2021. The inclusion criteria were: (1) postoperative pathologically confirmed gastric adenocarcinoma; (2) standard preoperative enhanced CT scan of the abdomen, including non-contrast phase, arterial phase (AP), and portal venous phase (PP) CT images; and (3) no other treatment prior to the CT examination. Exclusion criteria were: (1) incomplete clinical data and CT images; (2) tumors with a minimum diameter of less than 5 mm, making it difficult to outline the region of interest (ROI); and (3) poor image quality. Ultimately, 194 patients with gastric adenocarcinoma, comprising 139 males and 55 females, aged 29–86 years (mean age  $61.44 \pm 10.35$ ), were included. The flowchart of this study is shown in Fig. 1. The data were randomly divided into 137 cases in the training group and 57 cases in the validation group at a 7:3 ratio and were further divided into the VI group and the non-VI group based on pathology analysis. The training group included 31 VI cases and 106 non-VI cases, while the validation group included 12 VI cases and 45 non-VI cases.

### Clinical characteristics

Clinical data, including demographics and gastroscopic pathology, were gathered using picture archiving and communication systems (PACS). The demographic information included gender and age. The T stage was evaluated by the two senior radiologists with CT images. The gastroscopic pathological information included tumor location, Ki-67 labeling index (Ki-67), human epidermal growth factor receptor 2 (HER2), and Lauren classification.

### CT scanning protocol

Patients included in this study underwent abdominal CT examination after fasting for at least 6 h. Before the examination, patients were asked to drink an appropriate amount of water to expand the stomach. During the scan, patients were instructed to lie on their backs. A non-contrast CT scan was followed by an enhanced scan after injecting 80 ml of contrast agent iohexanol (350 mg/ml) through the cubital vein at a flow rate of 3.0 ml/s, followed by 20 ml of saline at a flow rate of 2.5 ml/s. The scanning parameters were as follows: 64 rows of detectors; beam collimation  $64 \times 0.62$  mm; spacing 0.983; 120 kV/250–300 mA; scanning thickness 5 mm; scanning spacing 5 mm. Contrast-enhanced CT scans in the AP and PP began at approximately 25–30 s and 60–70 s, respectively.

### Pathological and immunohistochemical evaluation

Referring to the WHO classification of gastrointestinal tumors [20], preoperative and postoperative histopathological specimens were retrospectively analyzed by senior pathologists experienced in gastrointestinal pathology.

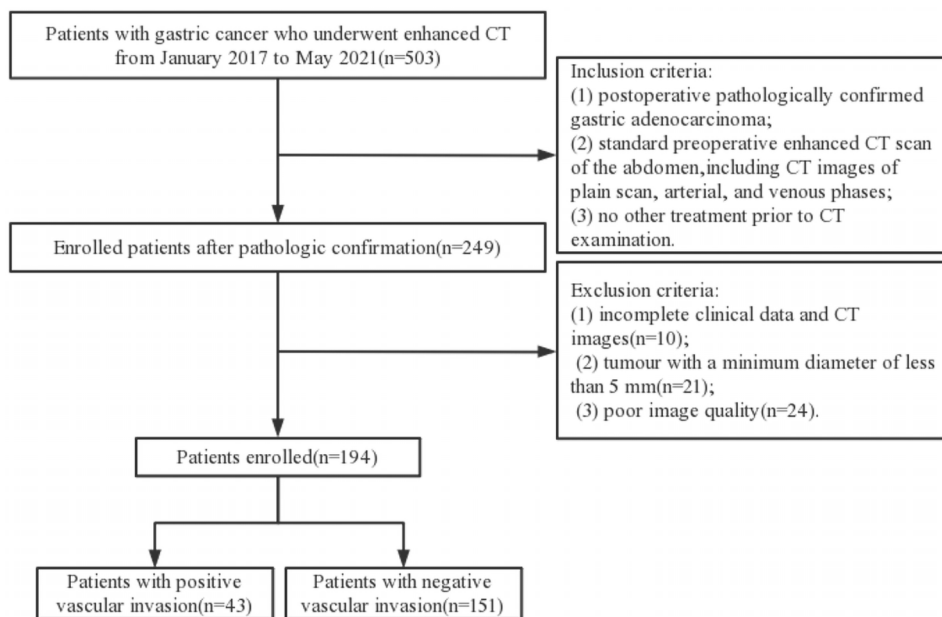


**Fig. 1** Flowchart for selecting patients



**Fig. 2** Sketch of the 3D segmentation of gastric cancer. **(A)** The sketch of manually delineating the region of interest (ROI) layer by layer in the arterial phase CT images by shrinking 2–3 mm along the tumor edge; **(B)** The sketch of manually delineating the region of interest (ROI) layer by layer in the portal venous phase CT images by shrinking 2–3 mm along the tumor edge; **(C)** 3D ROI of tumor

They assessed and recorded the vascular invasion status and Lauren classification of each patient's lesion. Ki-67 was assessed by calculating the percentage of positive nuclei relative to the total number of tumor nuclei in 10 high power fields (HPFs) per specimen, with positive staining defined as more than 50% of nuclei being positive and negative staining as 50% or fewer. For HER2 assessment, HER2 0 and HER2 1+ were defined as negative, and HER2 3+ as positive according to the guidelines [21]. Patients with HER2 2+ were excluded as they were not further analyzed by fluorescence in situ hybridization.

## Radiomics analysis of CT images

### Lesion segmentation

Two senior radiologists with experience in abdominal diagnosis evaluated the AP and PP CT images of each patient, assessing tumor size, location, and border, and reached a consensus. The AP and PP CT images of all patients were downloaded from the PACS and imported into ITK-SNAP software (Version 3.4.0, [http://www.](http://www.itksnap.org/)

[itksnap.org/](http://www.itksnap.org/)). The tumor was manually outlined layer by layer on the software platform by the two senior radiologists, using the location of the postoperatively recorded lesions as a guide. The ROI was kept as close as possible to the size of the lesion, with the outer edge maintained 2–3 mm from the tumor margin to avoid the influence of the gastric lumen. The final 3D ROI of the entire tumor lesion was automatically segmented by the software (Fig. 2).

### Feature extraction

All 3D ROI data and the original DICOM files were imported into A.K. software (Artificial Intelligence Kit, AI kit) for feature extraction. A total of 396 radiomics features were extracted, including: (1) histogram features: uniformity, kurtosis, etc.; (2) grey level co-occurrence matrix (GLCM) features: entropy, variance, etc.; (3) grey level run length matrix (GLRLM) features: short run emphasis, gray level nonuniformity, etc.; (4) gray level size zone matrix (GLSZM) features: small area emphasis,

large area emphasis, etc.; (5) shape parameter features: spherical volume ratio, compactness, etc.

### Feature preprocessing

The mean value of each feature obtained based on the 3D ROI outlined by the two radiologists was calculated. Anomalous feature parameters that turned out to be nan or Inf were excluded and replaced by the mean value. Each feature was normalized.

### Feature selection and Radiomics Model Building

The minimum redundancy maximum correlation (mRMR) algorithm was used to eliminate redundant and irrelevant features, retaining the top 30 features. The remaining features were then reduced and cross-validated using the least absolute shrinkage and selection operator (LASSO) regression algorithm. The features were combined with their corresponding regression coefficients in a weighted linear combination to calculate the radiomics score (Rad-Score). The clinical features and Rad-score were used to create a combined prediction model using logistic multiple regression, and a

nomogram and decision curve analysis (DCA) were completed. The study workflow is shown in Fig. 3.

### Statistical analysis

Statistical analysis was performed using R software (<https://www.r-project.org>, version 4.1.3) and SPSS 24.0 software (IBM, Armonk, NY, USA).  $P < 0.05$  was considered statistically significant. Measurement data following the normal distribution were expressed as mean  $\pm$  standard deviation (SD). The Mann-Whitney U-test was used to compare these variables. Categorical variables were expressed as median (first quartile, third quartile), and comparisons of categorical variables were made using the chi-squared test or Fisher's exact test. The intra-class correlation coefficient (ICC) was used to evaluate the consistency of outlining the ROI between the two senior radiologists. The ICC value was interpreted as follows: ICC < 0.20, slight agreement; ICC = 0.21–0.40, fair agreement; ICC = 0.41–0.60, moderate agreement; ICC = 0.61–0.80, substantial agreement; ICC = 0.81–1.0, almost perfect agreement. Clinical characteristics and radiomics parameters that were statistically significant

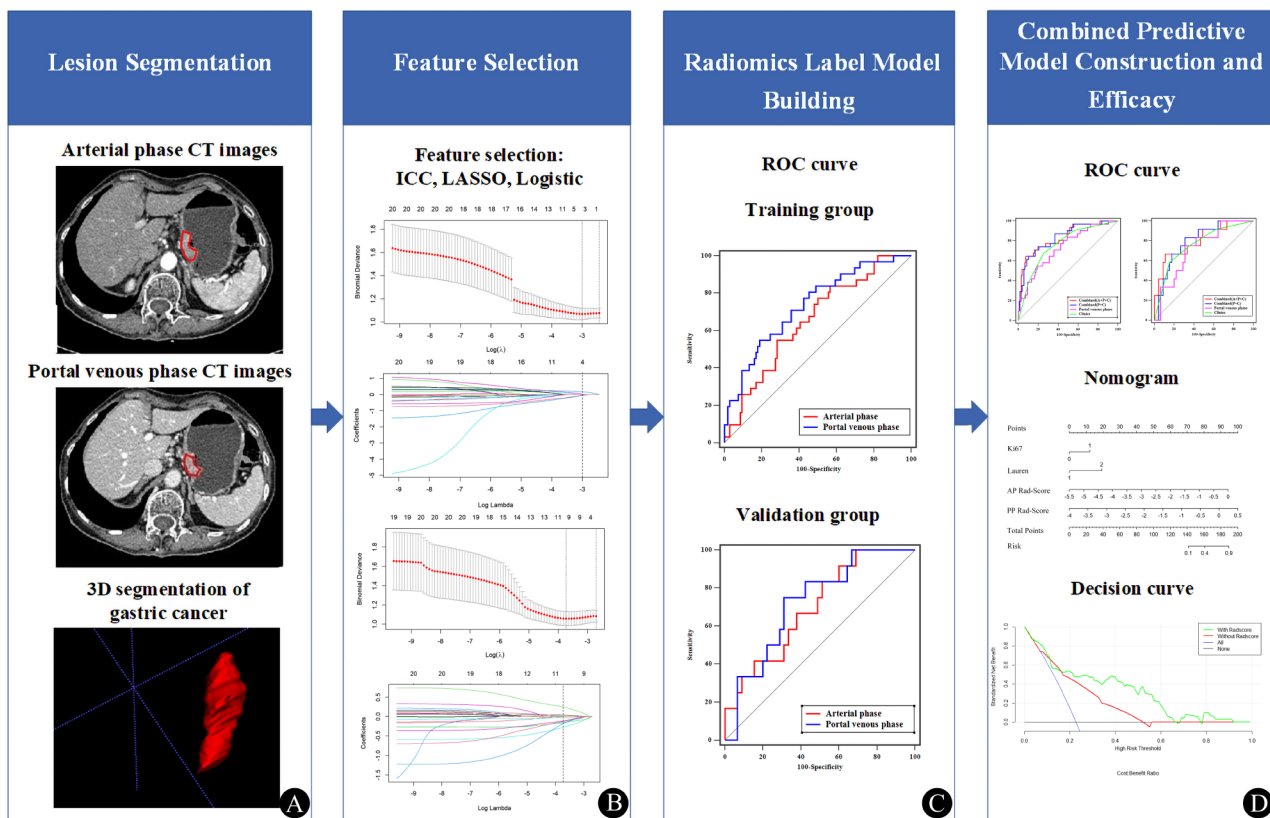


**Fig. 3** The workflow of the present study. **(A)** Contrast-enhanced CT imaging was acquired. The 3D segmentation were manually delineated around the entire tumor outline on each axial slice of arterial phase (AP) and portal venous phase (PP), and peritumoral shrinkage (2–3 mm) were automatically generated. **(B)** Feature selection was performed in the training cohort (AP and PP) based on the intraclass correlation coefficient (ICC) and least absolute shrinkage and selection operator (LASSO) binary logistic regression model. **(C)** Predictive models were constructed by multivariable logistic regression with the selected radiomics labels. **(D)** The AP and PP radiomics labels were selected to construct combined predictive model, followed by receiver operating characteristic (ROC) curve analysis, nomogram analysis, and decision curve analysis

were analyzed by multiple logistic regression. The diagnostic performance of each model was evaluated using receiver operating characteristic (ROC) curve analysis, and clinical benefit was assessed using decision curve analysis (DCA).

## Results

### Clinical characteristics

The clinical characteristics of the training and validation groups are summarized in Table 1. The VI group consisted of 43 cases, with 32 males and 11 females; 4 cases were in stage T2, 8 in stage T3, and 31 in stage T4a. The non-VI group comprised 151 cases, with 107 males and 44 females; 37 were in stage T1, 18 in stage T2, 34 in stage T3, and 62 in stage T4a. In this study, the intestinal and mixed types with better prognosis were combined into a group of 121 cases, and the diffuse type with worse prognosis was grouped into 73 cases. In patients with VI, Ki-67(+) and diffuse type were more common. There were no significant differences in age, gender, HER2, and tumor location between the VI and non-VI groups in both the training and validation groups.

### Radiomics feature analysis

Three radiomics features were randomly selected for ICC analysis, resulting in values of 0.994, 0.968, and 0.966, respectively, all with  $P < 0.001$ . After eliminating redundant and irrelevant features using the LASSO binary logistic regression algorithm, 4 features of AP and

9 features of PP remained (Fig. 4A-D). The features and corresponding coefficients for each phase are shown in Table 2.

**Table 2** Coefficient of selected radiomics characteristics

Group	Radiomics characteristics	Group	Coefficient
Arterial phase group	Zone Percentage	GLSZM	0.174
	LongRunLowGreyLevelEmphasis_All-Direction_offset2_SD	GLRLM	0.024
	ClusterShade_AllDirection_offset8_SD	GLCM	-0.045
Portal venous phase group	ShortRunLowGreyLevelEmphasis_All-Direction_offset8_SD	GLRLM	-0.058
	GLCMEntropy_angle135_offset7	GLCM	-0.031
	GLCMEntropy_angle135_offset4	GLCM	-0.156
	Low Intensity Small Area Emphasis	GLSZM	-0.113
	Mean Deviation	Histogram	-0.143
	Compactness1	Shape	-0.275
	ShortRunHighGreyLevelEmphasis_All-Direction_offset2_SD	GLRLM	-0.122
Portal venous phase group	Voxel Value Sum	Shape	0.038
	ShortRunEmphasis_angle0_offset1	GLRLM	0.255
	HaralickCorrelation_AllDirection_offset5_SD	GLCM	-0.181

GLCM, grey level co-occurrence matrix; GLRLM, grey level run length matrix; GLSZM, gray level size zone matrix

### Radiomics label model building and efficacy

Predictive models were constructed using multivariable logistic regression with the selected radiomics features.

**Table 1** Baseline characteristics of the patients in training and validation groups

Variable	Training group (n = 137)		P value	Validation group (n = 57)		P value
	VI (+) (n = 31)	VI (-) (n = 106)		VI (+) (n = 12)	VI (-) (n = 45)	
Age, mean ± SD, years	62.1 ± 10.27	61.14 ± 9.52	0.596	55.83 ± 14.09	63.13 ± 10.97	0.59
Gender, n (%)			0.637			1
Male	23(74.2%)	74(69.8%)		9(75.0%)	33(73.3%)	
Female	8(25.8%)	32(30.2%)		3(25.0%)	12(26.7%)	
Lauren classification			< 0.001*			0.043*
Diffuse type	22(71.0%)	29(27.4%)		8(66.7%)	14(31.1%)	
Intestinal and mixed type	9(29.0%)	77(72.6%)		4(33.3%)	31(68.9%)	
Ki-67			0.005*			0.022*
positive	22(71.0%)	45(42.5%)		8(66.7%)	13(28.9%)	
negative	9(29.0%)	61(57.5%)		4(33.3%)	32(71.1%)	
HER 2			0.442			0.261
positive	4(12.9%)	20(18.9%)		1(8.3%)	12(26.7%)	
negative	27(87.1%)	86(81.1%)		11(91.7%)	33(73.3%)	
Tumor location			0.358			0.12
Cardiac fundus and lower esophagus	1(3.2%)	9(8.5%)		0(0%)	0(0%)	
Gastric curvature	9(29.0%)	33(31.1%)		2(16.7%)	20(44.4%)	
Large curvature of the stomach	2(6.5%)	9(8.5%)		0(0%)	4(8.9%)	
Gastric antrum and pylorus	13(41.9%)	47(44.3%)		9(75.0%)	17(37.8%)	
Full stomach	6(19.4%)	8(7.5%)		1(8.3%)	4(8.9%)	

\* $P < 0.05$ ; VI vascular invasion

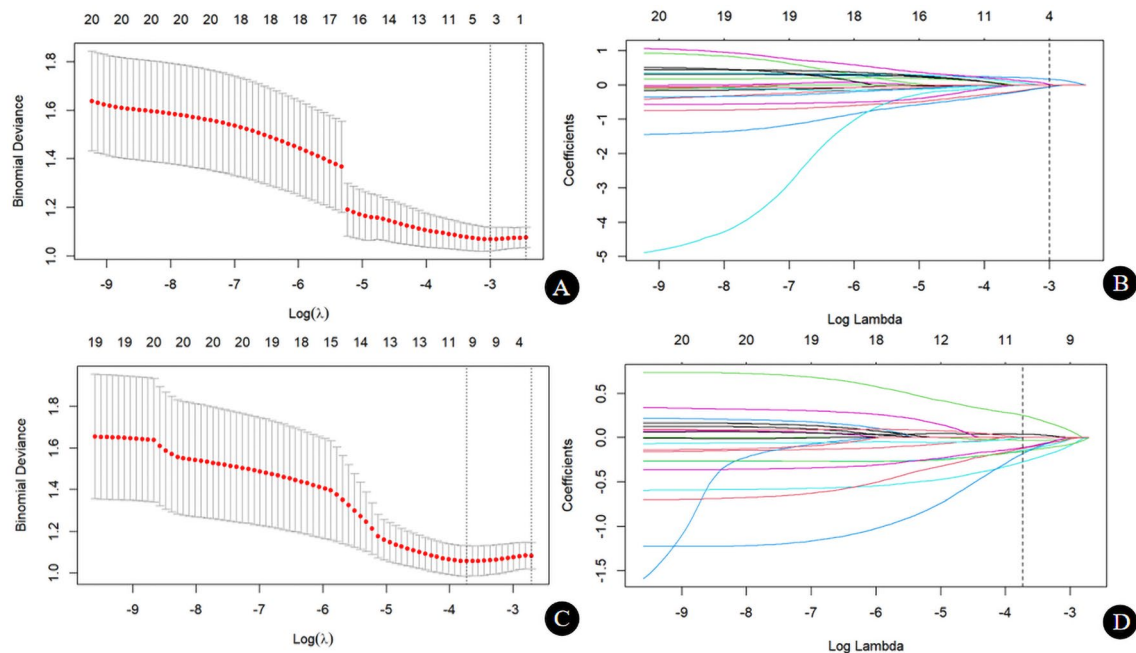


**Fig. 4** Radiomics feature selection based on the least absolute shrinkage and selection operator (LASSO) binary logistic regression model. **(A)** Ten-fold cross-validation via minimum criteria was used for tuning the parameter (lambda) in the LASSO model. The relationship between the binomial deviance and log (lambda) was plotted of arterial phase. **(B)** The LASSO coefficient profiles of the 396 radiomics features. A vertical line was drawn at the value selected using 10-fold cross-validation, where the optimal lambda resulted in 4 nonzero coefficients of arterial phase. **(C)** Ten-fold cross-validation via minimum criteria was used for tuning the parameter (lambda) in the LASSO model. The relationship between the binomial deviance and log (lambda) was plotted of portal venous phase. **(D)** The LASSO coefficient profiles of the 396 radiomics features. A vertical line was drawn at the value selected using 10-fold cross-validation, where the optimal lambda resulted in 9 nonzero coefficients of portal venous phase

**Table 3** Performance of the individualized prediction models

Models	AUC	95% CI	Sensitivity	Specificity	PPV	NPV
Training cohort						
A	0.65	0.57–0.73	77.42%	50%	60.76%	68.89%
P	0.73	0.65–0.80	54.84%	81.13%	74.40%	64.24%
C	0.76	0.68–0.83	67.74%	74.53%	72.67%	69.79%
P+C	0.83	0.76–0.89	64.52%	89.62%	86.14%	71.64%
A+P+C	0.83	0.76–0.89	64.52%	92.45%	89.50%	72.27%
Validation cohort						
A	0.70	0.56–0.81	83.33%	48.89%	61.98%	74.57%
P	0.72	0.58–0.83	75.00%	68.89%	70.68%	73.37%
C	0.76	0.63–0.87	58.33%	84.44%	78.94%	66.96%
P+C	0.80	0.67–0.89	83.33%	68.89%	72.82%	80.52%
A+P+C	0.80	0.67–0.89	66.67%	88.89%	85.72%	72.73%

Note A and P indicate the predicted model based on arterial phase images and portal venous phase images, respectively. C indicates the predicted model based on the combination of Ki-67 and Lauren classification. CI Confidence Interval

The AP and PP Rad-scores were calculated for each patient by linear combination of the selected radiomics features weighted by their respective coefficients in the predictive models. The predictive model based on AP images had an AUC value of 0.65 (95% CI 0.57–0.73) in the training group and 0.70 (95% CI 0.56–0.81) in the validation group. The predictive model based on PP images showed an AUC value of 0.73 (95% CI 0.65–0.80) in the training group and 0.72 (95% CI 0.58–0.83) in the validation group. A comparison of the two models in

the training and validation groups is shown in Table 3; Fig. 5A-B.

**Combined predictive model construction and efficacy**

A univariate regression analysis model of clinical parameters was performed to determine VI risk factors, identifying Ki-67 and Lauren classification as candidates. Although the AUC value of the AP prediction model was lower than that of the PP prediction model, the Rad-score of the AP prediction model was stable and

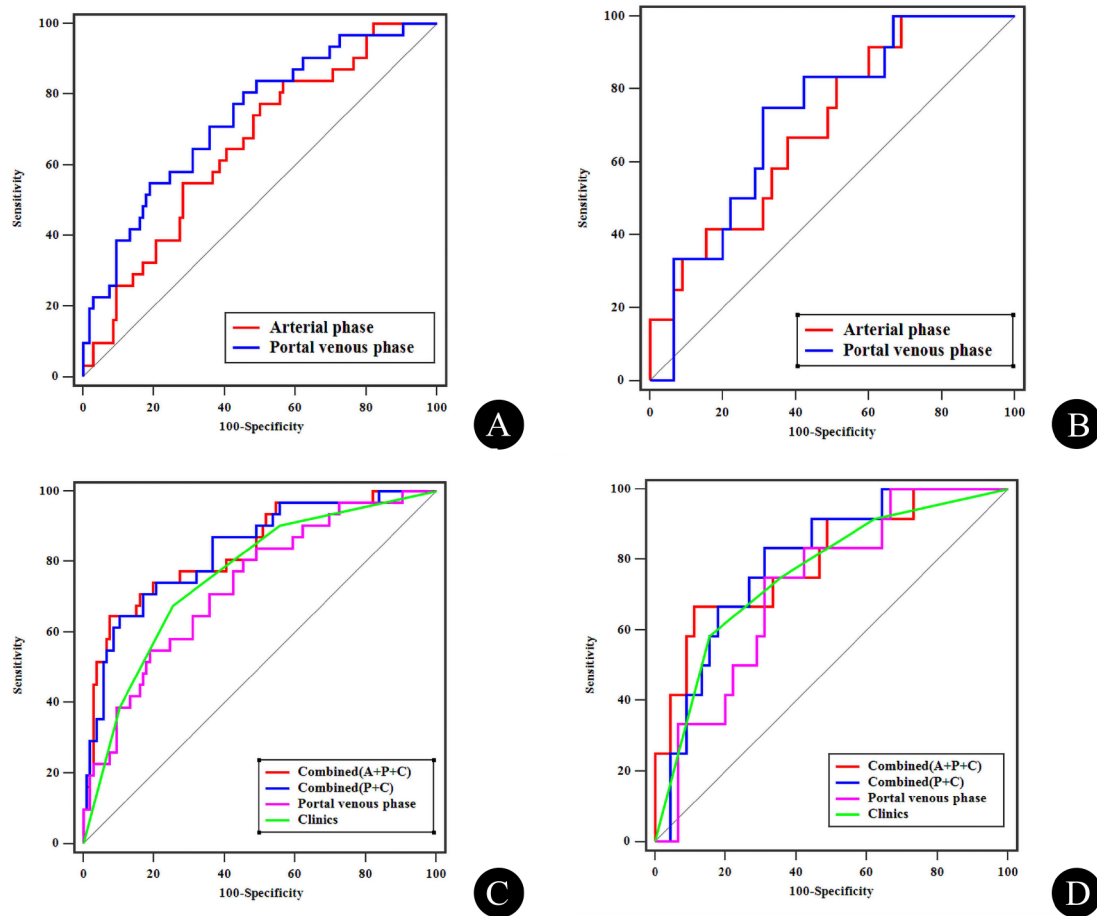


**Fig. 5** The efficiency of prediction models. **(A)** Receiver operating characteristics(ROC) curves for the radiomics label prediction model based on arterial phase(AP) and portal venous phase(PP) CT images respectively in the training cohort. **(B)** ROC curves for the radiomics label prediction model based on AP and PP CT images respectively in the validation cohort. **(C)** ROC curves for the radiomics label and clinical label prediction models and the ROC curves for the combined models in the training cohort. **(D)** ROC curves for the radiomics label and clinical label prediction models and the ROC curves for the combined models in the validation cohort

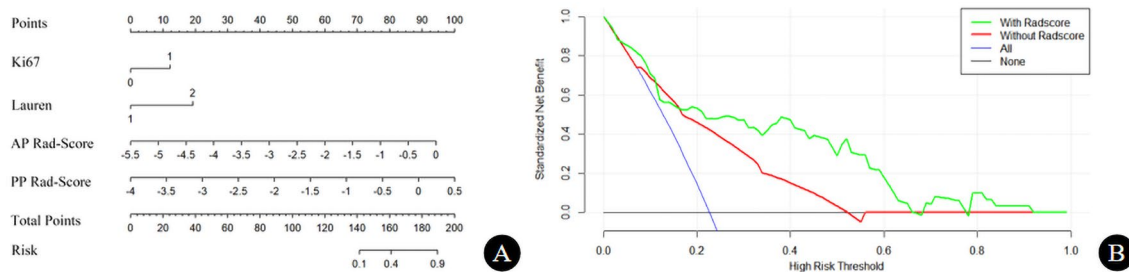


**Fig. 6** Nomogram and decision curve analysis curve of the combined prediction model based on arterial phase and portal venous phase CT images. **(A)** Nomogram; **(B)** Decision curve analysis curve, showing that the prediction model with radiomics features obtained more clinical benefits than without

had high sensitivity. Therefore, the Lauren classification and Ki-67 were combined with the Rad-scores (AP and PP) to construct a combined prediction model via multivariable logistic regression analysis. Nomogram was plotted based on the multiple logistic regression analysis (Fig. 6A) to quantitatively predict vascular invasion.

The ROC curves showed that in the combined prediction model based on clinical features and PP Rad-score (Fig. 5C-D), the AUC value for the training group was 0.83 (95% CI 0.76–0.89), with a sensitivity of 64.52% (95% CI 0.454–0.808) and specificity of 89.62% (95% CI 0.822–0.947); the AUC value for the validation group was 0.80 (95% CI 0.67–0.89), with a sensitivity of 83.33% (95% CI

0.516–0.979) and specificity of 68.89% (95% CI 0.534–0.818). The ROC curves also showed that the combined prediction model with the AP Rad-score was more stable than without it (Fig. 5C-D). The sensitivity and specificity for the training group were 64.52% (95% CI 0.454–0.808) and 92.45% (95% CI 0.857–0.967), respectively; for the validation group, the sensitivity and specificity were 66.67% (95% CI 0.349–0.901) and 88.89% (95% CI 0.759–0.963), respectively. The performance of the combined nomogram in the training cohort was significantly superior to that of the clinical model (AUC, 0.833 vs. 0.761,  $P=0.048$ ), while there was no significant difference between the models in the validation cohort (AUC, 0.800 vs. 0.763,  $P=0.228$ ). The DCA showed that the combined predictive model combining AP Rad-score and PP Rad-score had a greater net clinical benefit than the single clinical model (Fig. 6B).

## Discussion

The presence of vascular invasion (VI) is associated with worse clinical outcomes in patients with gastric cancer. In this study, we developed and validated a combined model based on enhanced CT images, Ki-67, and Lauren classification for the preoperative prediction of VI. We found that radiomics features based on arterial phase (AP) and portal venous phase (PP) CT images, converted into a quantitative Rad-score, could be independent predictors of VI. The combined model performed well in the prediction of VI (AUC=0.83), thereby providing an effective tool for prognosis prediction and clinical decision-making.

VI is associated with recurrence of gastric cancer, and the survival rate of patients with early recurrence is lower than that of patients with late recurrence [22]. Therefore, early detection of VI is crucial. However, obtaining and quantifying VI with conventional tools is challenging, as subjective assessment of images or pathological sampling biopsies can only assess a small part of the tumor [23]. In recent years, radiomics, aided by computer technology, has made it possible to detect internal tumor heterogeneity non-invasively and accurately [24]. Radiomics provides an objective and quantitative assessment of tumor heterogeneity by analyzing the values, distribution, and relationships of pixel or voxel grey levels in images [25, 26]. In our study, we developed two radiomics models based on AP images and PP images, respectively. We found that the prediction model based on PP images had better performance than the prediction model based on AP images, suggesting that radiomics features based on PP images might be more correlated with VI in gastric cancer, consistent with the findings of Fan et al. [27]. Despite this, the AP prediction model exhibited high sensitivity and stability. Incorporating the AP Rad-score into the combined predictive model improved its stability.

Previous studies have demonstrated that a high Ki-67 expression level is a risk factor for high survival risks [28]. Our results support this view. Meier A et al. [29] revealed that deep learning features based on enhanced CT images correlated with Ki-67 expression levels. Lauren classification of gastric cancer divides tumors into intestinal, diffuse, and mixed types based on histopathological characteristics, with the diffuse type having a worse prognosis [30]. Li et al. reported that Lauren classification is a risk factor for gastric cancer recurrence [31]. In our study, the Rad-score based on PP images achieved an AUC of 0.73, similar to the Clinical model (AUC=0.76). To improve the assessment and prediction of VI in gastric cancer, we combined pathological immunohistochemical indicators Ki-67 and Lauren classification with radiomics features to develop a combined predictive model. By incorporating Ki-67 and Lauren classification, the overall predictive ability was strong in both the training and validation groups, with AUCs of 0.83 and 0.80, respectively. Qiong et al. [23] developed radiomics and deep transfer learning prediction models based on contrast-enhanced CT imaging, yielding AUCs of 0.755 and 0.725 in the training and testing datasets. Both values were lower than those achieved by our combined prediction model.

HER2 overexpression initiates various signaling pathways leading to cellular proliferation and tumorigenesis [32]. In our study, there was no statistically significant difference in HER2 between the VI and non-VI groups, whereas a statistically significant difference in Ki-67 was observed between the groups. This discrepancy may be because Ki-67 expression serves as an indicator of active tumor cell proliferation. Stimulation of vascular endothelial growth factor causes small vessels to proliferate, increasing tumor vascular invasion. Consequently, Ki-67 is more sensitive than HER2 in detecting vascular invasion. Previous studies have also found Ki-67 to be associated with T stage, recurrence, and disease-free survival of gastric cancer [33, 34]. The Nomogram showed that higher Ki-67, Lauren classification as diffuse type, and higher Rad-score were associated with a greater likelihood of vascular invasion in gastric cancer.

We used 3D ROI for tumor segmentation in this study, which can comprehensively capture the biological characteristics of the whole tumor. 3D ROI is more comprehensive and accurate than 2D ROI [35]. In this study, meaningful, highly stable, and reproducible radiomics features such as GLCM, GLRLM, and shape parameters were screened out. GLCM features reflect the spatial correlation of image gray, and GLRLM features mainly reflect the directionality and roughness of image texture, indirectly indicating the heterogeneity of pathological changes [36]. These features could avoid subjective image interpretations by radiologists and serve as effective



auxiliary parameters in diagnosing vascular invasion in gastric cancer.

Chen et al. [37] described that the specificity of predictive models based on PP images was higher than the sensitivity. What's more, their work also showed that the specificity and sensitivity of predictive models based on T stage also had the same performance (specificity=0.816, sensitivity=0.480). Similarly, our combined prediction models showed high specificity and lower sensitivity. In our study, the specificity in the validation cohort of the combined predictive model based on PP Rad-score and clinical labels was 0.896, while it was 0.689 in the training cohort. We speculate this may be due to Ki-67 expression levels being associated with the T stage of gastric cancer or related to the unbalanced sample size between the VI and non-VI groups in this study [33]. In the subsequent research, we plan to enlarge the sample size to further validate the predictive model. We believe that specificity is more important for vascular invasion in gastric cancer, as it ensures the true-positive rate of prediction, preventing the inclusion of false-positive patients, and is more conducive to personalized clinical treatment.

There are some limitations in this study. Firstly, this study is retrospective and thus subject to selection bias. Secondly, it is a single-center and small sample study, and further validation with a large sample size and multiple centers is required in the future. Additionally, this study only considered the value of Lauren classification, Ki-67, HER2, and imaging features in predicting VI and did not consider the predictive value of tumor markers and other clinical indicators, which should be investigated further by including more indicators in the future.

## Conclusion

In conclusion, this study demonstrates the potential role of preoperative assessment of vascular invasion in gastric cancer through the application of radiomics analysis based on enhanced CT images, Ki-67, and Lauren classification. The integration of these imaging and pathological features into a combined predictive model enhances the accuracy and utility of preoperative evaluations, supporting more informed and tailored clinical decision-making for gastric cancer patients.

## Acknowledgements

We thank all patients who contributed to this study.

## Author contributions

All the authors have precipitated in the conception and design of the study. Conceptualization, Yi Liu and Kexin Zhu; methodology, Zhicheng Chen and Guangfeng Zhang; validation, Zhicheng Chen and Guangfeng Zhang; data analysis, Zhicheng Chen and Guangfeng Zhang; prepared figures, Zhicheng Chen; writing-original draft preparation, Zhicheng Chen and Guangfeng Zhang; writing- review and editing, Kexin Zhu; visualization and supervision, Yi Liu and Kexin Zhu. The author(s) read and approved the final manuscript.

## Funding

No funding.

## Data availability

The data are not publicly available due to them containing information that could compromise research participant privacy or consent but are available from the corresponding author on reasonable request.

## Declarations

### Ethics approval and consent to participate

This retrospective study was compliant with the Declaration of Helsinki, and was approved by the Ethics Committee of the First Hospital of China Medical University (No.2017-156-2). The written informed consent was waived by ethics committee of the First Hospital of China Medical University.

### Consent for publication

Not applicable.

### Competing interests

The authors declare no competing interests.

Received: 8 December 2022 / Accepted: 9 August 2024

Published online: 16 August 2024

## References

- Sung H, Ferlay J, Siegel RL, Laversanne M, Soerjomataram I, Jemal A, et al. Global Cancer statistics 2020: GLOBOCAN estimates of incidence and Mortality Worldwide for 36 cancers in 185 countries. *CA. Cancer J Clin.* 2021;71(3):209–49.
- Gao K, Wu J. National trend of gastric cancer mortality in China (2003–2015): a population-based study. *Cancer Commun.* 2019;39(1):24.
- Smyth EC, Nilsson M, Grabsch HI, van Grieken NC, Lordick F. Gastric cancer. *LANCET.* 2020;396(10251):635–48.
- Kim TU, Kim S, Lee NK, Kim HJ, Han GJ, Lee JW, et al. Prognostic value of computed tomography-detected extramural venous invasion to Predict Disease-Free Survival in patients with gastric Cancer. *J Comput Assist Tomogr.* 2017;41(3):430–6.
- Jacome AA, Coutinho AK, Lima EM, Andrade AC, Dos SJ. Personalized medicine in gastric cancer: where are we and where are we going? *World J Gastroenterol.* 2016;22(3):1160–71.
- Zhang CD, Ning FL, Zeng XT, Dai DQ. Lymphovascular invasion as a predictor for lymph node metastasis and a prognostic factor in gastric cancer patients under 70 years of age: a retrospective analysis. *INT J SURG.* 2018;53:214–20.
- Wang J, Zhong L, Zhou X, Chen D, Li R. Value of multiphase contrast-enhanced CT with three-dimensional reconstruction in detecting depth of infiltration, lymph node metastasis, and extramural vascular invasion of gastric cancer. *J Gastrointest Oncol.* 2021;12(4):1351–62.
- Li ZY, Tang L, Li ZM, Li YL, Fu J, Zhang Y, et al. Four-point computed tomography scores for evaluation of Occult Peritoneal Metastasis in patients with gastric Cancer: a region-to-region comparison with staging Laparoscopy. *ANN SURG ONCOL.* 2020;27(4):1103–9.
- Ghidini M, Vuozzo M, Galassi B, Mapelli P, Ceccarossi V, Caccamo L, et al. The role of Positron Emission Tomography/Computed tomography (PET/CT) for staging and Disease Response Assessment in Localized and locally Advanced Pancreatic Cancer. *Cancers (Basel).* 2021;13(16):4155.
- Sah BR, Owczarczyk K, Siddique M, Cook G, Goh V. Radiomics in esophageal and gastric cancer. *Abdom Radiol (NY).* 2019;44(6):2048–58.
- Xu Q, Sun Z, Li X, Ye C, Zhou C, Zhang L, et al. Advanced gastric cancer: CT radiomics prediction and early detection of downstaging with neoadjuvant chemotherapy. *EUR RADIOL.* 2021;31(11):8765–74.
- Chen Q, Zhang L, Liu S, You J, Chen L, Jin Z, et al. Radiomics in precision medicine for gastric cancer: opportunities and challenges. *EUR RADIOL.* 2022;32(9):5852–68.
- Dong D, Tang L, Li ZY, Fang MJ, Gao JB, Shan XH, et al. Development and validation of an individualized nomogram to identify occult peritoneal metastasis in patients with advanced gastric cancer. *ANN ONCOL.* 2019;30(3):431–8.

14. Liu Z, Wang S, Dong D, Wei J, Fang C, Zhou X, et al. The applications of Radiomics in Precision diagnosis and treatment of Oncology: opportunities and challenges. *THERANOSTICS*. 2019;9(5):1303–22.
15. Zhang W, Fang M, Dong D, Wang X, Ke X, Zhang L, et al. Development and validation of a CT-based radiomic nomogram for preoperative prediction of early recurrence in advanced gastric cancer. *RADIOTHER ONCOL*. 2020;145:13–20.
16. Wang Y, Liu W, Yu Y, Liu JJ, Xue HD, Qi YF, et al. CT radiomics nomogram for the preoperative prediction of lymph node metastasis in gastric cancer. *EUR RADIOL*. 2020;30(2):976–86.
17. Yang L, Chu W, Li M, Xu P, Wang M, Peng M, et al. Radiomics in Gastric Cancer: First Clinical Investigation to Predict Lymph Vascular Invasion and Survival Outcome using 18F-FDG PET/CT images. *Front Oncol*. 2022;12:836098.
18. Ko GH, Go SI, Lee WS, Lee JH, Jeong SH, Lee YJ, et al. Prognostic impact of Ki-67 in patients with gastric cancer—the importance of depth of invasion and histologic differentiation. *Med (Baltim)*. 2017;96(25):e7181.
19. Loughrey MB, Shepherd NA. The indications for biopsy in routine upper gastrointestinal endoscopy. *Histopathology*. 2021;78(1):215–27.
20. Nagtegaal ID, Odze RD, Klimstra D, Paradis V, Rugge M, Schirmacher P, et al. The 2019 WHO classification of tumours of the digestive system. *Histopathology*. 2020;76(2):182–8.
21. Shitara K, Bang YJ, Iwasa S, Sugimoto N, Ryu MH, Sakai D, et al. Trastuzumab Deruxtecan in previously treated HER2-Positive gastric Cancer. *N Engl J Med*. 2020;382(25):2419–30.
22. Kang WM, Meng QB, Yu JC, Ma ZQ, Li ZT. Factors associated with early recurrence after curative surgery for gastric cancer. *World J Gastroenterol*. 2015;21(19):5934–40.
23. Li Q, Feng QX, Qi L, Liu C, Zhang J, Yang G, et al. Prognostic aspects of lymphovascular invasion in localized gastric cancer: new insights into the radiomics and deep transfer learning from contrast-enhanced CT imaging. *Abdom Radiol (NY)*. 2022;47(2):496–507.
24. Lambin P, Leijenaar R, Deist TM, Peerlings J, de Jong E, van Timmeren J, et al. Radiomics: the bridge between medical imaging and personalized medicine. *NAT REV CLIN ONCOL*. 2017;14(12):749–62.
25. Rogers W, Thulasi SS, Refaee T, Lieverse R, Granzier R, Ibrahim A, et al. Radiomics: from qualitative to quantitative imaging. *Br J Radiol*. 2020;93(1108):20190948.
26. Avanzo M, Stancanello J, Pirrone G, Sartor G. Radiomics and deep learning in lung cancer. *STRAHLENTHER ONKOL*. 2020;196(10):879–87.
27. Fan L, Li J, Zhang H, Yin H, Zhang R, Zhang J, et al. Machine learning analysis for the noninvasive prediction of lymphovascular invasion in gastric cancer using PET/CT and enhanced CT-based radiomics and clinical variables. *ABDOM RADIOL*. 2022;47(4):1209–22.
28. Li N, Deng W, Ma J, Wei B, Guo K, Shen W, et al. Prognostic evaluation of nanog, Oct4, Sox2, PCNA, Ki67 and E-cadherin expression in gastric cancer. *MED ONCOL*. 2015;32(1):433.
29. Meier A, Nekolla K, Hewitt LC, Earle S, Yoshikawa T, Oshima T, et al. Hypothesis-free deep survival learning applied to the tumour microenvironment in gastric cancer. *J Pathology: Clin Res*. 2020;6(4):273–82.
30. Pernet S, Terme M, Radosevic-Robin N, Castan F, Badoual C, Marcheteau E, et al. Infiltrating and peripheral immune cell analysis in advanced gastric cancer according to the Lauren classification and its prognostic significance. *Gastric Cancer*. 2020;23(1):73–81.
31. Li P, He HQ, Zhu CM, Ling YH, Hu WM, Zhang XK, et al. The prognostic significance of lymphovascular invasion in patients with resectable gastric cancer: a large retrospective study from Southern China. *BMC Cancer*. 2015;15:370.
32. Oh DY, Bang YJ. HER2-targeted therapies - a role beyond breast cancer. *NAT REV CLIN ONCOL*. 2020;17(1):33–48.
33. Pyo JS, Kim NY. Meta-analysis of prognostic role of Ki-67 labeling index in gastric carcinoma. *Int J Biol Markers*. 2017;32(4):e447–53.
34. Seo SH, Kim KH, Oh SH, Choi Y, Ahn KJ, Lee JY, et al. Ki-67 labeling index as a prognostic marker in advanced stomach cancer. *ANN SURG TREAT RES*. 2019;96(1):27–33.
35. Fields B, Demirjian NL, Hwang DH, Varghese BA, Cen SY, Lei X, et al. Whole-tumor 3D volumetric MRI-based radiomics approach for distinguishing between benign and malignant soft tissue tumors. *EUR RADIOL*. 2021;31(11):8522–35.
36. Ekert K, Hinterleitner C, Horger M. Prognosis assessment in metastatic gastrointestinal stromal tumors treated with tyrosine kinase inhibitors based on CT-texture analysis. *EUR J RADIOL*. 2019;116:98–105.
37. Chen X, Yang Z, Yang J, Liao Y, Pang P, Fan W, et al. Radiomics analysis of contrast-enhanced CT predicts lymphovascular invasion and disease outcome in gastric cancer: a preliminary study. *Cancer Imaging*. 2020;20(1):24.

## Publisher's Note

Springer Nature remains neutral with regard to jurisdictional claims in published maps and institutional affiliations.